Anat Sci Int (2017) 92:554–568
DOI 10.1007/s12565-016-0361-y

ORIGINAL ARTICLE

Anatomy, histology and elemental profile of long bones and ribs of the Asian elephant (*Elephas maximus*)

Korakot Nganvongpanit[1,2] · Puntita Siengdee[1] · Kittisak Buddhachat[1] · Janine L. Brown[3] · Sarisa Klinhom[2] · Tanita Pitakarnnop[1] · Taweepoke Angkawanish[4] · Chatchote Thitaram[2]

Received: 7 April 2016 / Accepted: 26 July 2016 / Published online: 4 August 2016

Abstract This study evaluated the morphology and elemental composition of Asian elephant (*Elephas maximus*) bones (humerus, radius, ulna, femur, tibia, fibula and rib). Computerized tomography was used to image the intraosseous structure, compact bones were processed using histological techniques, and elemental profiling of compact bone was conducted using X-ray fluorescence. There was no clear evidence of an open marrow cavity in any of the bones; rather, dense trabecular bone was found in the bone interior. Compact bone contained double osteons in the radius, tibia and fibula. The osteon structure was comparatively large and similar in all bones, although the lacuna area was greater ($P < 0.05$) in the femur and ulna. Another finding was that nutrient foramina were clearly present in the humerus, ulna, femur, tibia and rib. Twenty elements were identified in elephant compact bone. Of these, ten differed significantly across the seven bones: Ca, Ti, V, Mn, Fe, Zr, Ag, Cd, Sn and Sb. Of particular interest was the finding of a significantly larger proportion of Fe in the humerus, radius, fibula and ribs, all bones without an open medullary cavity, which is traditionally associated with bone marrow for blood cell production. In conclusion, elephant bones present special characteristics, some of which may be important to hematopoiesis and bone strength for supporting a heavy body weight.

Keywords Bone · CT scan · Elephant · Mineral · Osteon

Abbreviations

Mg	Magnesium (12)
Al	Aluminum (13)
Si	Silicon (14)
P	Phosphorus (15)
S	Sulfur (16)
K	Potassium (19)
Ca	Calcium (20)
Ti	Titanium (22)
V	Vanadium (23)
Cr	Chromium (24)
Mn	Manganese (25)
Fe	Iron (26)
Ni	Nickel (28)
Cu	Copper (29)
Zn	Zinc (30)
Zr	Zirconium (30)
Ag	Silver (47)
Cd	Cadmium (48)
Sn	Tin (50)
Sb	Antimony (51)
pb	Lead (82)
LE	Light element from H = hydrogen (1) to Na = sodium (11)

✉ Korakot Nganvongpanit
korakot.n@cmu.ac.th

[1] Animal Bone and Joint Research Laboratory, Department of Veterinary Biosciences and Public Health, Faculty of Veterinary Medicine, Chiang Mai University, Chiang Mai 50100, Thailand

[2] Faculty of Veterinary Medicine, Center of Excellence in Elephant Research and Education, Chiang Mai University, Chiang Mai 50100, Thailand

[3] Smithsonian Conservation Biology Institute, Center for Species Survival, 1500 Remount Road, Front Royal, VA 22630, USA

[4] National Elephant Institute, Forest Industry Organization, Hangchat, Lampang 52190, Thailand

Introduction

Elephants are the largest land mammals and can weigh 5000 kg or more, raising interesting questions about how they functionally can support such weight. This is especially relevant in light of evidence that foot and joint problems occur in captive elephants (Lewis et al. 2010), particularly those that spend time on hard surfaces (Miller et al. 2016). Studies of the anatomy and physiology of elephant bone, and their load bearing characteristics, are of interest from a comparative standpoint and also could improve our understanding of how flooring substrate and exercise factors affect the health and welfare of ex situ populations.

Bone strength is reliant on a dense network of organized collagen and mineralization and is determined by the trabecular microstructure and density of compact bone, both of which are affected by the elemental constituents therein (Seeman 2006) and forces that act on the bone (Hammer 2015). Studies on bone structure of elephants are limited and have focused primarily on the macroanatomy, for example, that of the forelimb (Smuts and Bezuidenhout 1993), hindlimb (Smuts and Bezuidenhout 1994; Shil et al. 2013), skull (van der Merwe et al. 1995; Todd 2010) and foot (Weissengruber et al. 2006; Hutchinson et al. 2011). Curtin used synchrotron X-ray microtomography (SR-μCT) to study the histology of femoral and tibial diaphyses in extinct and extant elephantids (Curtin et al. 2012), finding that patterns of early bone growth were similar to those of other tetrapods that grow into large adults. But, in general, micro- and macroanatomical studies of elephant bone are few.

Several techniques have been used to study elements in biological samples, such as inductively coupled plasma mass spectrometry (IC-PMS) (Amr 2011), atomic absorption spectroscopy (ASS) (Fischer et al. 2013) and X-ray fluorescence (XRF) (Nganvongpanit et al. 2015a; Buddhachat et al. 2016a, b). We chose to use handheld XRF to analyze the elemental composition of elephant bones because this technique is noninvasive and nondestructive to samples. XRF has been used to provide information on the elemental components of various organic sample types, such as bone, teeth, horn and antlers (Christensen et al. 2012; Kierdorf et al. 2014; Nganvongpanit et al. 2015a, 2016a; Buddhachat et al. 2016a, b), including teeth and bone in elephants (Christensen et al. 2012; Kierdorf et al. 2014; Nganvongpanit et al. 2015a, 2016a; Buddhachat et al. 2016a, b).

The aim of this study was to characterize the histology and elemental composition of Asian elephant (*Elephas maximus*) long bones (humerus, radius, ulna, femur, tibia, fibula and 5th rib) using XRF, computerized tomography and histology to better understand the distinctive physiology of elephants and perhaps gain insight into how their bones are capable of supporting a high body weight.

Materials and methods

Bone samples

Long bones (humerus, radius, ulna, femur, tibia and fibula) and 5th ribs of five Asian elephant skeletons from two facilities were used in this study. Two elephants from the Animal Anatomy Museum, Department of Veterinary Biosciences and Public Health, Faculty of Veterinary Medicine, Chiang Mai University, Thailand, were used to study the intraosseous anatomy and elemental composition. Three elephant skeletons from the National Elephant Institute, Forest Industry Organization, Hangchat, Lampang, Thailand, were used for the histological study, in which small pieces of bone were removed by permission. Although exact ages of the skeletons were not known, all specimens were considered adult.

Intraosseous anatomy study

In this study, the humerus ($n = 2$), radius ($n = 2$), ulna ($n = 2$), femur ($n = 2$), tibia ($n = 2$), fibula ($n = 2$) and 5th rib ($n = 2$) of two female Asian elephants were used. To examine the intraosseous anatomy, computerized tomography scans (CT scans) were performed using a 16-slice scanner (Brilliance CT-16 slice, Philips) under the following conditions: 0.4 s tube rotation time, 120 kVp, 200 mA, 3 s/slice and 0.5 mm slice thickness. Data were analyzed using an image analyzing system (Software Version 2.2.1/22.5 Brilliance™, Philips).

Bones were weighed, and the thickness of compact and cancellous bones and diameter of each bone were measured by CT scans and averaged across bone types. A cancellous index (CI) was calculated using the diameter of each bone divided by the cancellous bone diameter; thus, a lower CI indicated increased cancellous bone thickness.

Histological study

In this study, the humerus ($n = 3$), radius ($n = 3$), ulna ($n = 3$), femur ($n = 3$), tibia ($n = 3$), fibula ($n = 3$) and 5th rib ($n = 3$) from three Asian elephants (sex unknown) were used. Samples were processed using conventional histological techniques as previously described (Nganvongpanit et al. 2015c). Bones (1.0–2.0 cm thickness) were cross-sectioned at the mid shaft point. Tissues were fixed in 10 % formalin for 24 h and then decalcified by 10 % nitric acid for 8 h. The specimens were cut into 1-mm pieces and

placed in plastic cassettes and then processed in 10 % formalin for 1 h (two changes), 95 % ethanol for 1 h (three changes), absolute isopropyl alcohol for 1 h (two changes), xylene for 1 h (two changes) and paraplast for 1 h (three changes). The tissues were then embedded in paraffin and cut into 5-μm sections.

Sections were deparaffinized in xylene and rehydrated through an ascending series of 95 % alcohols to water. Tissue sections were stained with Harris's hematoxylin for 5 min and washed under running tap water for 5 min; differentiated in 1 % acid alcohol (1 % hydrochloric acid in 70 % ethanol) for 5 s and washed under tap water for 5 min; dipped in saturated lithium carbonate solution for 5 s and washed under tap water for 5 min; stained with 1 % eosin Y for 3 min and washed under running tap water for 5 min. The sections were then dehydrated through 95 % alcohol and absolute alcohol, cleared in xylene and mounted in Permount.

Individual sections were observed using a compound light microscope (AxioCam; Carl Zeiss, Oberkochen, Germany) and measured using AxioVision 4.8.2 software. For each bone sample, at least 50 secondary osteons were measured from a series of six slides. Only mature osteons were measured. The diameter and area of Haversian canals and osteons and area of lacuna were determined. Because some of the Haversian canals and osteons were oval-shaped rather than circular, Haversian canal and osteon diameters were calculated by: [maximum diameter + minimum diameter]/2. Other characteristics of osteons, such as presence of a double cement line or plexiform bone, also were recorded. Data for all bone parameters were averaged across bone type.

Elemental measurements

In this study, the humerus ($n = 4$), radius ($n = 4$), ulna ($n = 4$), femur ($n = 4$), tibia ($n = 4$), fibula ($n = 4$) and 5th rib ($n = 4$) from two female Asian elephants were used. Evaluation of the elemental composition of bone samples was conducted using a Handheld XRF analyzer (DELTA Premium, Olympus, USA) with a silicon drift detector that detected elements from magnesium (Mg) through bismuth (Bi) on the periodic table. Light elements (LE) were those with an atomic number lower than Mg (H-Na) and could not be differentiated as separate elements. The collimator size was set at 0.3 mm for analysis-area diameter, and operating voltages of 10 and 40 kV, 2 min, were used as the source of incident radiation. Twenty separate sites on each bone were measured for elemental composition. Elemental values are presented as percentages of the total. A Ca/P ratio, the components of calcium hydroxyapatite, was calculated for each bone type (Christensen et al. 2012; Kierdorf et al. 2014; Zougrou et al. 2014).

Statistical analyses

Differences in measured bone parameters in the intraosseous anatomy and histology studies were determined by one-way ANOVA and Tukey's post hoc tests. Differences in elemental concentrations and elemental ratios between samples were determined by one-way ANOVA followed by post hoc multiple comparisons using LSD tests. Data are presented as mean ± SD, and P values <0.05 were considered statistically significant.

Results

Intraosseous anatomy study

Images are representative computerized topographic scans of the seven bones of Asian elephants using two- (Fig. 1) and three-dimensional (Fig. 2) imaging. A typical open medullary cavity was not found in any of the bones; rather the shaft was filled with cancellous bone. Moreover, using three-dimensional modeling, the cancellous bone appeared to be particularly compact (Fig. 3). Nutrient foramina were clearly observed in the humerus, ulna, femur, tibia and rib as shown in Fig. 4, which averaged 0.5 ± 0.1 mm in diameter.

The thickness of compact bone, cancellous bone and overall bone diameter is shown in Table 1. In general, the humerus had the greatest bone diameter and compact bone thickness, whereas ribs had the lowest ($P < 0.05$). Ribs also had the lowest cancellous bone thickness, similar to the fibula and radius. Femur had the thickest cancellous bone, which was similar to that of humerus and tibia. The relationship between bone diameter and cancellous bone thickness remained constant, as reflected by similar TI index values across bone types (Table 1).

Average weights of the femur, humerus, ulna, tibia, radius, rib and fibula were 6.20 ± 0.29, 4.99 ± 0.22, 2.71 ± 0.21, 2.20 ± 0.16, 0.74 ± 0.09, 0.47 ± 0.09 and 0.33 ± 0.09 kg, respectively. All differed ($P < 0.01$), except for the rib and fibula, which were similar ($P = 0.07$).

Histology

Representative histological sections from Asian elephant bones are shown in Fig. 5, with associated measurements of the Haversian canals, osteons and lacunae presented in Table 2. The lacuna area was greatest in the femur followed by the ulna when compared to the other five bones. In ribs, 20 % of the osteons were over 100,000 μm^2 in area, which we refer to as super osteons as compared to

Fig. 1 Sagittal and frontal of topogram from computerized tomographic scan images of the humerus (**a**), ulna (**b**), radius (**c**), femur (**d**), tibia and fibula (**e**) and rib (**f**) of Asian elephants. The cortical bones are the most dense structures and are radiopaque. The cancellous bones are less dense structures and are slightly radiopaque. The physeal scar of the bone is a thin radiopaque line perpendicular to the long axis of bone. Not presenting a larger radiolucent area inside the bone along the axis of the bone means the medullary cavity is absent

Fig. 2 Sagittal and frontal computed tomographic scan image using three-dimensional imaging of the femur, humerus, ulna, radius, tibia, fibula and rib (*H* head/proximal, *F* foot/distal, *A* anterior/cranial, *P* posterior/caudal, *R* right/lateral, *L* left/median). *White color* represents a cortical bone while *orange color* represents a cancellous bone

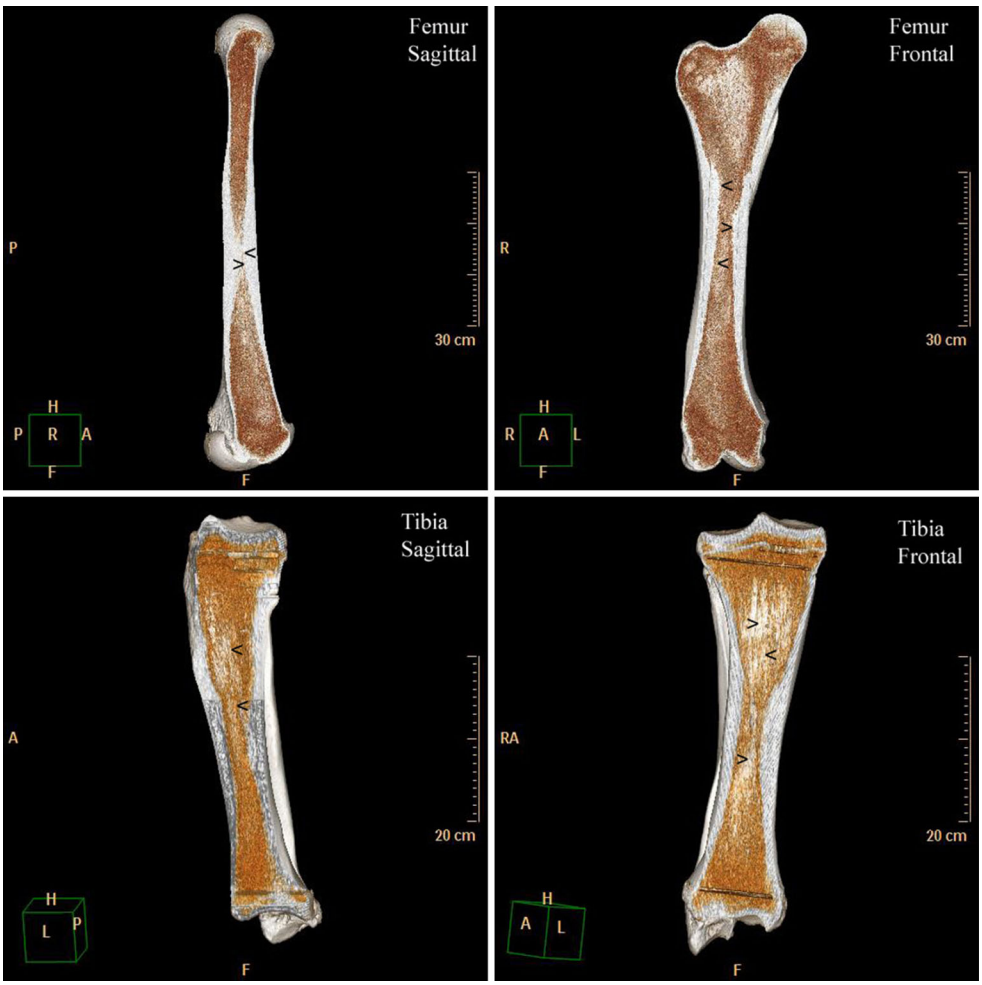

Fig. 3 Sagittal and frontal computed tomographic scan images using three-dimensional modeling of femur (*top panels*) and tibia (*bottom panels*) bones of the Asian elephant. *Arrowheads* indicate area of compact bone fill in intraosseous cancellous bone (*H* head/proximal, *F* foot/distal, *A* anterior/cranial, *P* posterior/caudal, *R* right/lateral, *L* left/median)

average osteon size. Compact bone in elephants contained secondary osteon structures and double cement lines in the radius, tibia and fibula bone. These double cement lines are hypercalcified rings within the lamellae in a mature osteon (Fig. 6). The ratios between osteons with single and double cement lines were 6:1, 12:1 and 24:1 in the radius, tibia and fibula bone, respectively. Plexiform bone was not found in any of the bone types.

Elemental profile and ratios

Distribution of the 20 elements plus LE detected in the seven bones (Al, Si, P, S, K, Ca, Ti, V, Cr, Mn, Fe, Ni, Cu, Zn, Zr, Ag, Cd, Sn, Sb and Pb) for all data combined is shown in Fig. 7. Only four of these elements (Ca, P, Si and LE) were above 1 %, with LE being the highest, followed by Ca, P and Si (Fig. 7a). All others were at a concentration less than 1 % (Fig. 7b). Of those, Fe was present in the highest proportion, followed by Al, K and S, with all others constituting very small percentages. Three elements were not found in every bone: K was only found in the radius; Ni was not found in femur, tibia or fibula; Cu was not found in humerus or fibula (Fig. 8). LEs also were not found in the ulna. Of the 20 detectable elements, nine (Al, Si, P, S, Cr, Ni, Cu, Zn, Pb) were present in similar concentrations ($P > 0.05$) among the seven bones (Fig. 8).

Ten elements differed significantly across the bone types (Fig. 9). For example, Ca was highest in the femur and lowest in the radius bone ($P < 0.05$). Titanium differed ($P < 0.05$) among four bones: it was highest in the fibula and lowest in the tibia. V was highest in the rib and lowest in the femur and tibia ($P < 0.05$). Mn was significantly ($P < 0.05$) higher in the fibula and lower in the femur. Fe was present in significantly higher amounts in the humerus, radius, fibula and rib compared with the femur, ulna and tibia. Zr was higher ($P < 0.05$) in the fibula and lower in the femur and tibia. Ag, Cd, Sn and Sb were lower ($P < 0.05$)

Fig. 4 Sagittal and frontal topogram from computed tomographic scan images of the humerus, ulna, femur, tibia and rib showing the radiolucent line as the nutrient foramen (*arrowhead*)

Table 1 Mean (± SD) and mean range (min, max) measurements of the bone diameter, cancellous bone thickness, compact bone thickness and cancellous bone index at the diaphysis of long bones and ribs from three Asian elephants

	Bone diameter (cm)	Cancellous bone thickness (cm)	Compact bone thickness (cm)	Cancellous bone index
Humerus	10.13 ± 1.18^{d} (8.67, 12.31)	$5.15 \pm 1.11^{b,c}$ (3.39, 7.28)	2.49 ± 0.51^{c} (1.94, 3.39)	2.0 ± 0.4^{c}
Radius	3.34 ± 0.51^{b} (2.40, 4.27)	1.80 ± 0.39^{a} (1.19, 2.31)	0.77 ± 0.19^{b} (0.54, 1.14)	$1.9 \pm 0.3^{b,c}$
Ulna	6.76 ± 0.63^{c} (5.88, 8.14)	4.11 ± 0.48^{b} (3.64, 4.82)	1.32 ± 0.21^{c} (1.12, 1.74)	$1.7 \pm 0.1^{a,b}$
Femur	$8.70 \pm 3.09^{c,d}$ (4.77, 15.17)	6.07 ± 2.50^{c} (2.92, 11.47)	1.32 ± 0.53^{c} (0.64, 2.31)	1.5 ± 0.3^{a}
Tibia	7.43 ± 1.25^{c} (5.55, 9.89)	$4.36 \pm 1.37^{b,c}$ (2.41, 6.55)	1.53 ± 0.34^{c} (0.99, 2.07)	$1.8 \pm 0.4^{a,b,c}$
Fibula	2.72 ± 0.37^{b} (2.15, 3.32)	1.40 ± 0.41^{a} (0.88, 2.25)	0.66 ± 0.09^{b} (0.49, 0.74)	$2.0 \pm 0.4^{b,c}$
Rib	0.26 ± 0.02^{a} (0.22, 0.27)	0.16 ± 0.03^{a} (0.12, 0.19)	0.05 ± 0.01^{a} (0.04, 0.07)	$1.6 \pm 0.2^{a,b}$

^{a,b,c,d} Mean values within columns are significantly different ($P < 0.05$)

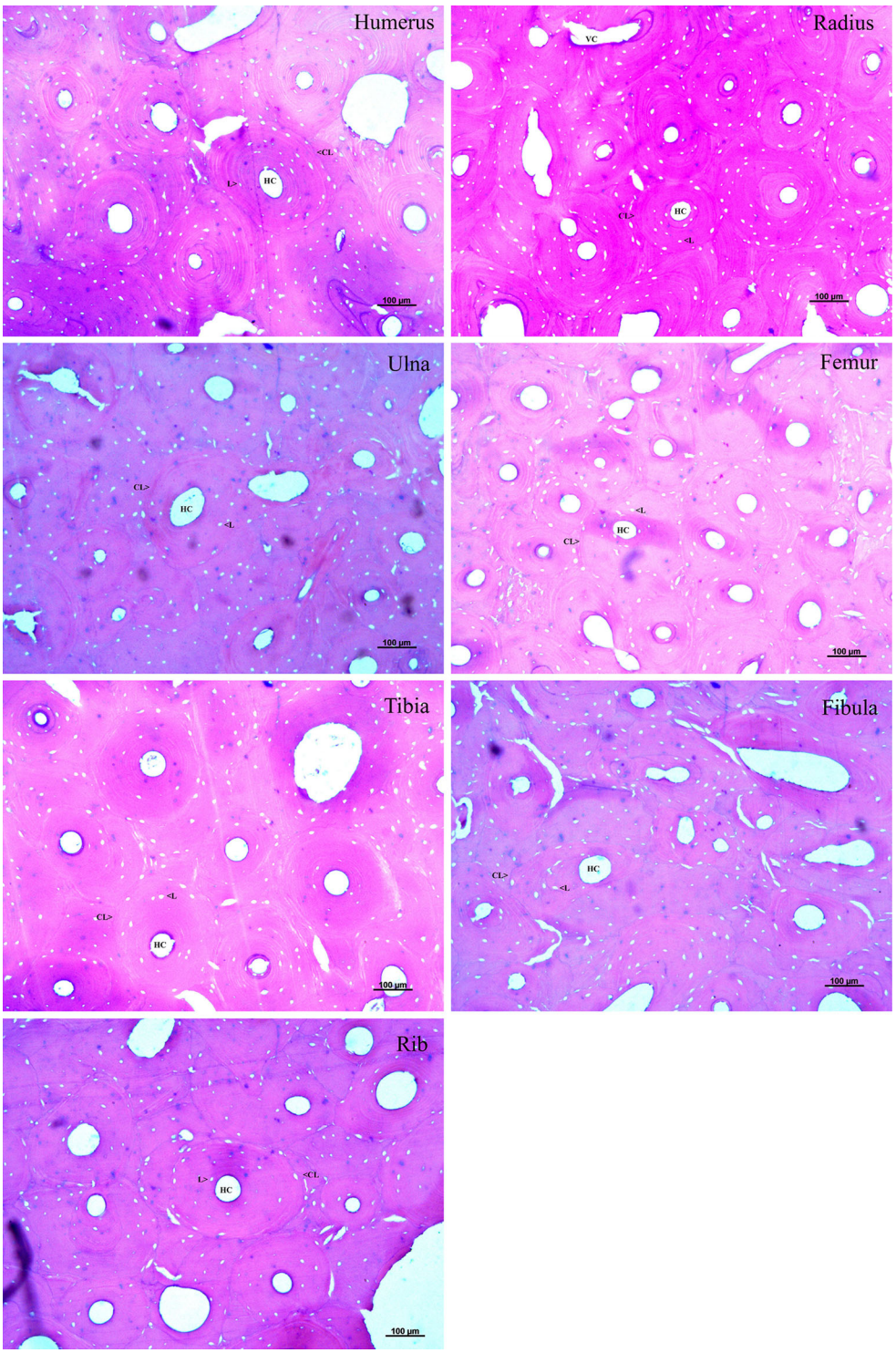

Fig. 5 Representative photomicrographs of hematoxylin and eosin-stained transverse sections of compact bone from the humerus, radius, ulna, femur, tibia, fibula and rib of the Asian elephant (magnification ×50). *CL* cement line, *HC* Haversian canal, *L* lacuna, *V* Volkman's canal

in the femur than in the humerus and fibula. Potassium was not included in Figs. 8 or 9 because this element was found only in the radius (0.390 ± 0.218 ppm). The Ca/P ratio across all bones ranged from 2.59 to 2.82 with no significant differences (Fig. 10).

Discussion

In this study, we characterized the intraosseous anatomy of long bones and ribs in the adult Asian elephant and the associated histology and elemental profiles. Based on CT

Table 2 Mean (± SD) and mean range (min, max) measurements of the diameter and area of the Haversian canal and osteon, lacuna area and number of lacuna/osteons of long bones and ribs from three Asian elephants

	Haversian canal		Osteon		Lacuna area (μm^2)	Number of lacuna/osteon
	Diameter (μm)	Area (μm^2)	Diameter (μm)	Area (μm^2)		
Humerus	56 ± 20^{a} (21, 97)	$3326 \pm 3388^{a,b}$ (487, 19,200)	233 ± 78^{a} (72, 421)	$6200 \pm 7677^{b,c}$ (3997, 434,330)	90 ± 60^{e} (3, 543)	$15 \pm 6^{a,b}$ (4, 30)
Radius	$61 \pm 24^{a,b}$ (260, 113)	2876 ± 2013^{a} (488, 8862)	$262 \pm 72^{a,b}$ (166, 469)	$4498 \pm 2,268^{a,b}$ (15,727, 113,967)	$85 \pm 62^{b,c}$ (3, 730)	$13 \pm 6^{a,b}$ (1, 32)
Ulna	$72 \pm 31^{b,c}$ (26, 126)	$4590 \pm 3076^{a,b}$ (460, 13,950)	$269 \pm 62^{a,b}$ (125, 459)	$4949 \pm 2020^{a,b,c}$ (9961, 101,732)	103 ± 83^{d} (5, 748)	16 ± 9^{b} (4, 43
Femur	$62 \pm 23^{a,b,c}$ (20, 134)	$3754 \pm 2966^{a,b}$ (436, 12,570)	243 ± 69^{a} (122, 443)	$4853 \pm 3238^{a,b,c}$ (10,614, 136,910)	134 ± 119^{e} (4, 949)	$15 \pm 7^{a,b}$ (1, 36)
Tibia	$74 \pm 21^{a,b,c}$ (37, 130)	3756 ± 2092^{a} (776, 9458)	235 ± 59^{a} (101, 389)	$3814 \pm 2,335^{a}$ (7146, 146,344)	76 ± 53^{a} (2, 436)	12 ± 7^{a} (2, 38)
Fibula	$67 \pm 29^{a,b,c}$ (21, 140)	3241 ± 2710^{a} (514, 15,846)	212 ± 95^{a} (78, 455)	$3364 \pm 2,997^{a,b}$ (4718, 128,043)	$74 \pm 59^{a,b}$ (3, 494)	$11 \pm 7^{a,b}$ (2, 39)
Rib	75 ± 21^{c} (35, 136)	5167 ± 5703^{b} (754, 41,173)	296 ± 120^{b} (118, 720)	$7090 \pm 8,321^{c}$ (5549, 589,771)	$85 \pm 64^{a,b,c}$ (4, 733)	$15 \pm 8^{a,b}$ (3, 42)

^{a,b,c,d,e} Mean values within columns are significantly different ($P < 0.05$)

scans, the humerus, radius, ulna, femur, tibia, fibula and rib in Asian elephants did not appear to have a marrow cavity such as that found in other species (Frandson et al. 2009; Houssaye et al. 2015), including humans (Netter 2014). Rather, elephant bone consisted of outer compact bone filled with trabecular bone, which in the femur and tibia was particularly dense. In most mammalian species, the femur is the longest and heaviest bone, whereas the tibia is the principal weight bearer of the hindlimbs, a relationship found in African elephants (Smuts and Bezuidenhout 1994). In our study, we also found the femur was the heaviest bone, followed by the humerus. However, the ulna was larger than the radius, which differs from other species, such as dog, cat, horse and pig, where the radius is more weight bearing (Frandson et al. 2009). Typically, the majority of weight in a quadruped is borne by the front legs, while the rear legs provide propulsion. Elephants bear about 55 % of the weight on the forelimbs (Panagiotopoulou et al. 2012), with a more vertical orientation in the hindlimb. Thus, the weight on the hindlimb is more direct, while forelimb weight is distributed because of the angle of the shoulder and elbow (Smuts and Bezuidenhout 1993, Smuts and Bezuidenhout 1994; Shil et al. 2013). We suggest that the presence of dense trabecular bone in the intraosseous region of the femur and tibia is important for bone strength.

Another finding from the histology study was the presence of double cement lines, or double-zoned, secondary osteons, which exhibited a hypercalcified ring within the lamellae of the osteon. This ring is thought to reflect a slowing or temporary cessation of infilling during osteon formation. Double-zoned osteons were first described in human bone in 1974 (Pankovich et al. 1974) and were suggested to be the result of an abrupt change in mineral density or one or more growth arrest lines, or as a result of intraosteonal remodeling of an existing secondary osteon and aging (Pankovich et al. 1974; Skedros et al. 2007). Interestingly, double cement lines have not been reported in animals, including dog, cat, rat, horse, pig, buffalo, cow, goat, sheep, deer and monkey (Mori et al. 2003; Martiniaková et al. 2006; Hillier and Bell 2007; Skedros et al. 2007; Nganvongpanit et al. 2015b). However, we found double cement lines in the radius, tibia and fibula bones of Asian elephant, with the radius having the highest ratio (6:1) compared with the tibia (12:1) and then fibula (24:1). The purpose of double-zoned osteons in elephant bone is unclear, but it might be significant in that elephants, like humans, are a long-lived species. Interestingly, although all skeletons were from mature animals, in some images, a metaphyseal line was evident, suggestive of incomplete epiphyseal fusion normally found in young animals. However, a previous report did find metaphyseal lines in adult elephant limb bones of living and fossil specimens,

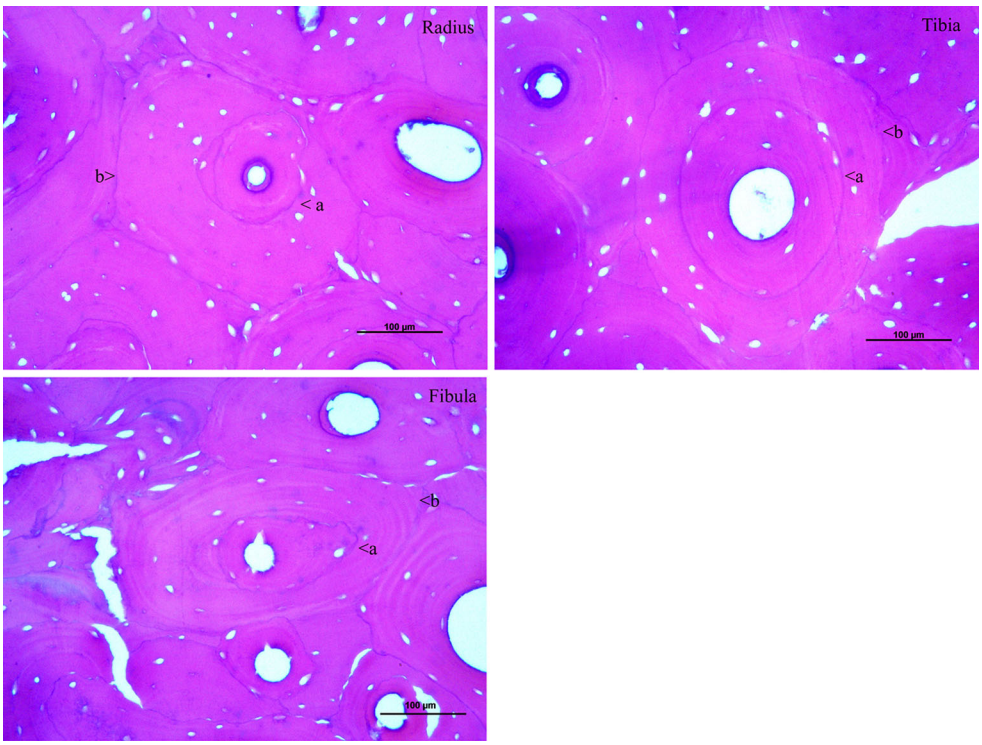

Fig. 6 Representative photomicrographs of hematoxylin and eosin-stained transverse sections of compact bone from the radius, tibia and fibula of Asian elephants with secondary osteons that exhibited a hypercalcified ring (**a**) within the lamellae of the osteon (**b**) (magnification ×100)

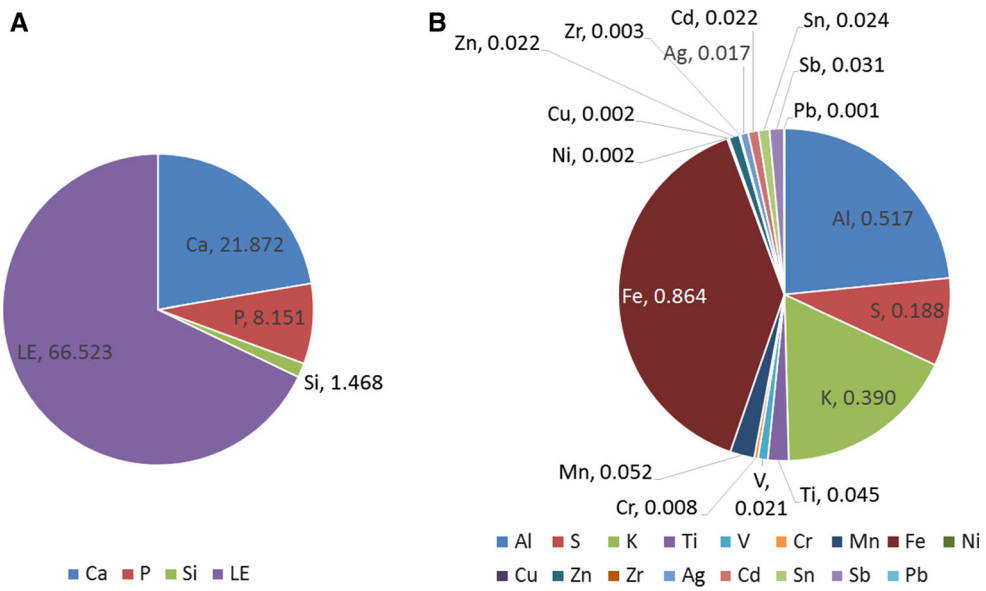

Fig. 7 Composition of elements found in long bones and ribs of the Asian elephant, data combined. Elements in concentration over 1 % are presented in **a**, whereas elements with concentration lower than 1 % are presented in **b**. Element abbreviations: aluminum (Al), silicon (Si), phosphorus (P), sulfur (S), potassium (K), calcium (Ca), titanium (Ti), vanadium (V), chromium (Cr), manganese (Mn), iron (Fe), nickel (Ni), copper (Cu), zinc (Zn), zirconium (Zr), silver (Ag), cadmium (Cd), tin (Sn), antimony (Sb) and lead (Pb)

with complete epiphyseal fusion later in ontogeny (Roth 1984).

Plexiform bone is characteristic of cortical bone in large and/or fast-growing animals, such as horses, pigs, buffalo, cows, goats and dogs, and it occurs with less frequency in primates, including humans and monkeys (Mori et al. 2003; Martiniaková et al. 2006; Hillier and Bell 2007; Nganvongpanit et al. 2015b). In some species, such as dog, sheep and deer, plexiform bone is found only in immature animals (Hillier and Bell 2007; Nganvongpanit et al. 2016b). None of the bones of Asian elephants in our study contained plexiform bone, which may be because they were all from adult elephants. A previous study in juvenile African and Asian elephants reported the presence of plexiform bone in femur and tibia (Curtin et al. 2012); thus, additional studies are needed to determine whether or how age affects bone

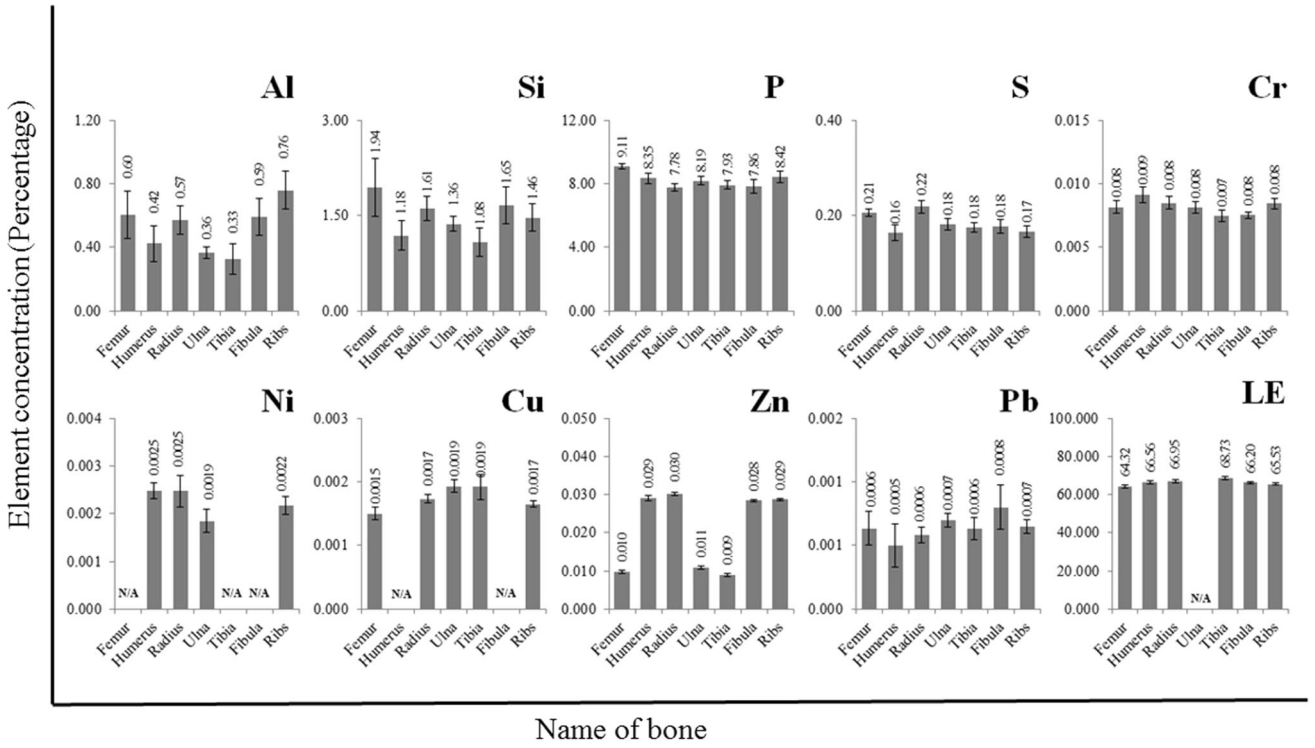

Fig. 8 Night elements including aluminum (Al), silicon (Si), phosphorus (P), sulfur (S), chromium (Cr), nickel (Ni), copper (Cu), zinc (Zn) and lead (Pb) and a light element (LE), which did not differ significantly in concentration across the long bones and ribs of Asian elephants. *N/A* Element was not detected

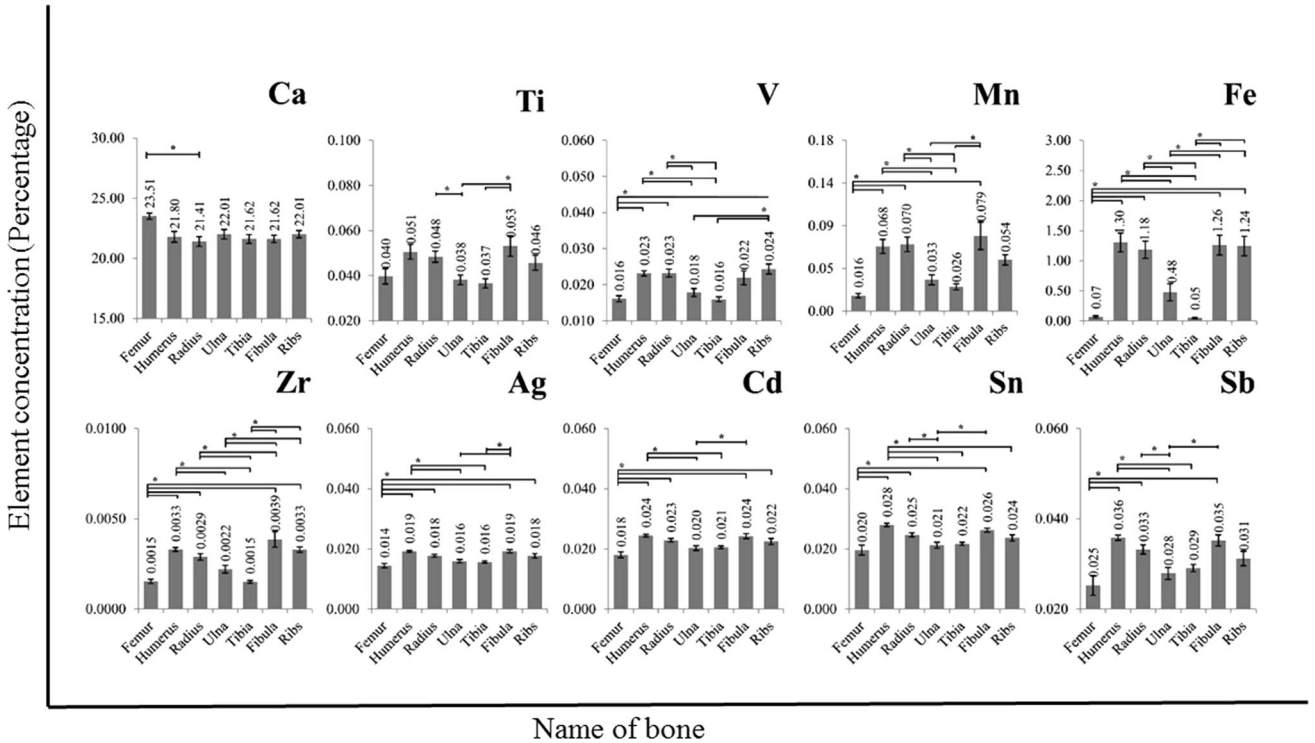

Fig. 9 Ten elements including; calcium (Ca), titanium (Ti), vanadium (V), manganese (Mn), iron (Fe), zirconium (Zr), silver (Ag), cadmium (Cd), tin (Sn) and antimony (Sb), which differed significantly in concentration across the long bones and ribs of Asian elephants ($*P < 0.05$)

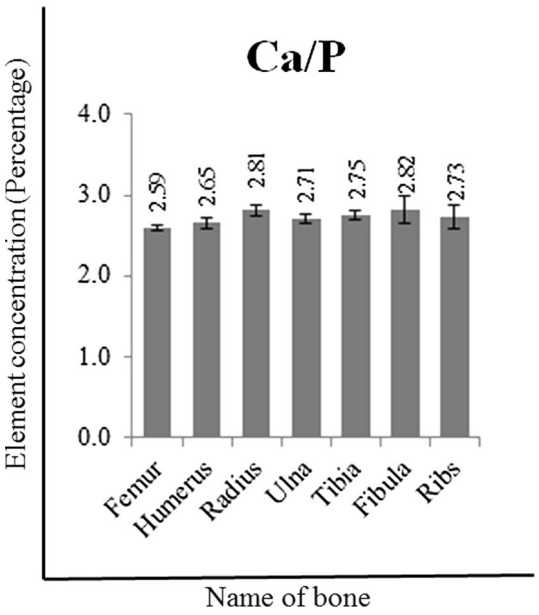

Fig. 10 Differences in the calcium (Ca)/phosphorus (P) ratio of Asian elephant long bones and ribs. All ratios did not significantly differ ($P > 0.05$) between bone types

structure in elephants and whether the physiological mechanisms are similar to those of other species.

In accordance with its size, the osteon structure in elephant compact bone was larger than that of other species. In comparing the osteon and Haversian canal diameter of tibia bone to that of other species (human, monkey, dog, cat, swine, cattle, chicken), the largest were found in the elephant and the smallest in the chicken (Table 3). Moreover, the number of osteocytes in elephant was low compared with other species, as shown in Table 4.

With respect to the elemental profiles, ten differed significantly among the seven bones. Calcium levels were the highest in the femur and lowest in the radius bone, although the Ca/P ratio was not different between these and the other bones examined. In all bones, the Ca/P ratios (Fig. 10) averaged 2.72, which was higher than the ratio of cabrbonate (CO_3^{2-}) to phosphate (PO_4^{3-}) in hydroxyapatite (2.15) (Wopenka and Pasteris 2005; Rey et al. 2009) and the bones of other mammals, such as human (2.21) (Tzaphidou and Zaichick 2004), pig (2.17) (Dickerson 1962), bovines (1.69) (Legros et al. 1987) and rat (1.65–2.18) (Dickerson 1962; Legros et al. 1987). It is possible a higher Ca/P ratio is needed to provide strength to elephant bones in light of the proportionally high weight they carry, although not all of these bones are weight bearing (e.g., ribs, fibula). Three other elements essential to bone metabolism, V, Mn and Fe, were higher in the humerus, radius, fibula and rib and lower in the femur, ulna and tibia bones, as were Zn, Ti, V, Mn, Fe and Zr. Iron plays an essential role in hematopoiesis; in long bones, it is principally stored in the bone marrow, but is also found in the liver and spleen bound to ferritin protein (Bessis and Breton-Gorius 1962). Of particular interest was the finding of a significantly larger proportion of Fe in the humerus, radius, fibula and ribs, all bones without an open marrow cavity, which is traditionally associated with blood cell production. Comparing Fe in the humerus bone across several bovid and cervid species, higher amounts were found in Asian elephants (Buddhachat et al. 2016a). This, in addition to our finding that major large nutrient foramens (one per bone) were present in the humerus, ulna, femur, tibia and rib of Asian elephant bone, suggests these bones may play a role in the production of hematopoietic cells, although the source of the cells in elephant is unclear (Mikota 2006). Thus, it could represent a species difference in bone function and hematopoiesis and warrants further study.

Table 3 Comparison of Harversian canal and osteon diameters (mean ± SD) of tibia bones from eight species

Species	Osteon diameter (μm)	Haversian canal diameter (μm)
Asian elephant	234.50 ± 58.94[a]	73.58 ± 21.48[a]
Human	111.07 ± 2.25[b]	35.92 ± 2.12[b]
	184.66 ± 28.63[c]	39.71 ± 7.95[c]
Monkey	143.46 ± 26.80[c]	33.74 ± 6.53[c]
Dog	59.39 ± 3.63[b]	12.37 ± 1.91[b]
	157.01 ± 32.87[d]	34.93 ± 9.06[d]
Cat	49.93 ± 3.29[b]	10.60 ± 1.01
Swine	114.76 ± 8.19[b]	40.09 ± 14.82[b]
Cattle	118.34 ± 16.40[b]	26.24 ± 3.75[b]
Chicken	45.73 ± 4.66[b]	29.49 ± 2.18[b]

[a] Data from current study

[b] Data from Morales et al. (2012)

[c] Data from Nganvongpanit et al. (2015b)

[d] Data from Nganvongpanit et al. (2016b)

Table 4 Comparison of the number of osteocytes per osteon (count lacuna as representative of osteocytes in osteon) between Asian elephant and six other species

	Asian elephant[a]	Human[b]	Cat[b]	Sheep[b]	Deer[b]	Wolf[b]	Armadillo[b]
Humerus	15	49	35	67	52	62	N.A.
Radius	13	57	38	45	N.A.	N.A.	N.A.
Ulna	16	54	38	N.A.	41	N.A.	N.A.
Femur	15	51	38	64	N.A.	61	36
Tiba	12	48	38	42	N.A.	N.A.	39

N.A. data not available

[a] Data from current study

[b] Data from Horni (2002)

Copper is an essential trace element, involved in bone growth and strength, and deficiencies can result in deformed bones and increased bone fractures (Dollwet and Sorenson 1988). Copper was found in femur, radius, ulna, tibia and rib bones, but not humerus or fibula. Little is known about differential Cu distribution among different bone types, nor have specific Cu pathways been identified in elephants, so it is unclear whether Cu is an essential trace element in elephant bone. Metals such as Ti and Zr were present in all bones, but accumulation differed across types. However this element is not considered a non-essential element in bone, although its function is unclear (Dermience et al. 2015). Four heavy metals (Ag, Cd, Sn and Sb) were unevenly distributed, being highest in the humerus and fibula and lowest in the femur, which may be related to a higher blood supply for humerus bone. Previous studies showed heavy metals accumulated more in cancellous bone than compact bone because of a higher blood supply (Brodziak-Dopierała et al. 2015; Nganvongpanit et al. 2016a). We found Sn was low while Ca was high in femur and might be related. In rats (Yamaguchi et al. 1982), oral administration of Sn decreased Ca content in bone. Nickel is an essential nutrient with a role in membrane metabolism (Nielsen et al. 1989; Nielsen 1991; Poonkothai and Vijayavathai 2012) and was found in humerus, radius, ulna and rib bones. In 2011, Chovancová reported an effect of Ni on the macroscopic and microscopic structure of femoral bone tissue in rats, with intraperitoneal administration of $NiCl_2$ inducing changes in cortical bone thickness and compact bone microstructure (Chovancová et al. 2011). The finding of heavy metals, such as Cd and Pb, in elephant bones suggests the animals were exposed to environmental contamination during their lifetime, which has been found in other mineralized tissues in elephants (Christensen et al. 2012; Kierdorf et al. 2014; Nganvongpanit et al. 2015a, 2016a; Buddhachat et al. 2016a, b). Main sources of Pb contamination in Thailand are lead-based fuels, spent ammunition and wastewater (Chongsuvivatwong et al. 2011; Chanpiwat and Sthiannopkao 2014; Parkpian et al. 2003).

In conclusion, elephant long bones differ from those of other species in that there is no clear open marrow cavity as observed in other species. Elephant bone also was characterized by a large osteon structure and few osteocytes per osteon as compared to other species, which could mean most of the elephant bone is extracellular matrix. Finally, the Ca/P ratio was high compared to other species, which could be important for bone strength.

Acknowledgments The authors are grateful for research funding from the Chiang Mai University (CMU) through the research administration office, which provided a budget to the Center of Excellence in Elephant Research and Education.

Authors' contribution KN. is a major contributor and designed and conducted all the experiments. K.N. and S.K. scanned all samples in this study using XRF. K.N. performed the CT scans and histology of compact bone. T.P. measured the osteon structures. C.T. and T.A. gave advice and supplied rare samples used in this study. K.N., K.B. and P.S. analyzed all data and performed statistical analysis. K.N, K.B. and J.B. assisted in discussions and writing of the manuscript. All authors read and approved the manuscript to published.

Compliance with ethical standards

Ethical approval No ethical approval was required for this study.

Conflict of interest The authors report no conflicts of interest. The authors alone are responsible for the content and writing of the paper.

References

Amr AM (2011) Trace elements in Egyptian teeth. Int J Phys Sci 6:6241–6245

Bessis MC, Breton-Gorius J (1962) Iron metabolism in the bone marrow as seen by electron microscopy: a critical review. Blood 19:635–663

Brodziak-Dopierała B, Kwapuliński J, Sobczyk K, Wiechuła D (2015) Analysis of the content of cadmium and zinc in parts of the human hip joint. Biol Trace Elem Res 163:73–80

Buddhachat K, Klinhom S, Siengdee P et al (2016a) Elemental analysis of bone, teeth, horn and antler in different animal species using non-invasive handheld X-ray fluorescence. PLoS One 11:e0155458

Buddhachat K, Thitaram C, Brown JL et al (2016b) Use of handheld X-ray fluorescence as a non-invasive method to distinguish between Asian and African elephant tusks. Sci Rep 6:24845

Chanpiwat P, Sthiannopkao S (2014) Status of metal levels and their potential sources of contamination in Southeast Asian rivers. Environ Sci Pollut Res Int 21:220–223

Chongsuvivatwong V, Kaeosanit S, Untimanon O (2011) Twenty-six tons of lead oxide used per year in wooden boat building and repairing in southern Thailand. Environ Geochem Health 33:301–307

Chovancová H, Martiniaková M, Omelka R, Grosskopf B, Toman T (2011) Structural changes in femoral bone tissue of rats after intraperitoneal administration of nickel. Pol J Environ Stud 20:1147–1152

Christensen AM, Smith MA, Thomas RM (2012) Validation of X-ray fluorescence spectrometry for determining osseous or dental origin of unknown material. J Forensic Sci 57:47–51

Curtin AJ, Macdowell AA, Schaible EG, Roth VR (2012) Noninvasive histological comparison of bone growth patterns among fossil and extant neonatal elephantids using synchrotron radiation X-ray microtomography. J Vertebr Paleontol 32:939–955

Dermience M, Lognay G, Mathieu F, Goyens P (2015) Effects of thirty elements on bone metabolism. J Trace Elem Med Biol 32:86–106

Dickerson JW (1962) The effect of development on the composition of a long bone of the pig, rat and fowl. Biochem J 82:47–55

Dollwet HH, Sorenson JR (1988) Roles of copper in bone maintenance and healing. Biol Trace Elem Res 18:39–48

Fischer A, Wiechuła D, Przybyła-Misztela C (2013) Changes of concentrations of elements in deciduous teeth with age. Biol Trace Elem Res 154:427–432

Frandson RD, Wilke WL, Fails AD (2009) Anatomy and physiology of farm animals. Wiley-Blackwell, Iowa

Hammer A (2015) The paradox of Wolff's theories. Ir J Med Sci 184:13–22

Hillier ML, Bell LS (2007) Differentiating human bone from animal bone: a review of histological methods. J Forensic Sci 52:249–263

Hori H (2002) The forensic application of comparative mammalian bone histology. Texas Tech University, Texas, p 82

Houssaye A, Fernandez V, Billet GJ (2015) Hyperspecialization in some South American endemic ungulates revealed by long bone microstructure. J Mammal Evol October 28:1–15

Hutchinson JR, Delmer C, Miller CE, Hildebrandt T, Pitsillides AA, Boyde A (2011) From flat foot to fat foot: structure, ontogeny, function, and evolution of elephant "sixth toes". Science 334:1699–1703

Kierdorf U, Stoffels D, Kierdorf H (2014) Element concentrations and element ratios in antler and pedicle bone of yearling red deer (*Cervus elaphus*) stags-a quantitative X-ray fluorescence study. Biol Trace Elem Res 162:124–133

Legros R, Balmin N, Bonel G (1987) Age-related changes in mineral of rat and bovine cortical bone. Calcif Tissue Int 41:137–144

Lewis KD, Shepherdson DJ, Owens TM, Keele M (2010) A survey of elephant husbandry and foot health in North American zoos. Zoo Biol 29:221–236

Martiniaková M, Grosskopf B, Vondráková M, Omelka R, Fabis M (2006) Differences in femoral compact bone tissue microscopic structure between adult cows (*Bos taurus*) and pigs (*Sus scrofa* domestica). Anat Histol Embryol 35:167–170

Mikota SK (2006) Hemolymphatic system. In: Fowler ME, Mikota SK (eds) Biology, medicine, and surgery of elephants. Blackwell, Iowa, pp 325–345

Miller MA, Hogan JN, Meehan CL (2016) Housing and demographic risk factors impacting foot and musculoskeletal health in African elephants [Loxodonta africana] and Asian elephants [Elephas maximus] in North American zoos. PLoS One 11:e0155223

Morales JP, Roa HI, Zavando D, Suazo GI (2012) Determination of the species from skeletal remains through histomorphometric evaluation and discriminant analysis. Int J Morphol 30:1035–1041

Mori R, Kodaka T, Sano T, Yamagishi N, Asari M, Naito Y (2003) Comparative histology of the laminar bone between young calves and foals. Cells Tissues Organs 175:43–50

Netter FH (2014) Atlas of human anatomy. Saunders Elsevier, Philadelphia

Nganvongpanit K, Brown JL, Buddhachat K, Somgird C, Thitaram C (2015a) Elemental analysis of Asian elephant (*Elephas maximus*) teeth using X-ray fluorescence and a comparison to other species. Biol Trace Elem Res 170:94–105

Nganvongpanit K, Phatsara M, Settakorn J, Mahakkanukrauh P (2015b) Differences in compact bone tissue microscopic structure between adult humans (*Homo sapiens*) and Assam macaques (*Macaca assamensis*). Forensic Sci Int 254:e1–e5

Nganvongpanit K, Buddhachat K, Brown JL (2016a) Comparison of bone tissue elements between normal and osteoarthritic pelvic bones in dogs. Biol Trace Elem Res 171:344–353

Nganvongpanit K, Pradit W, Pitakarnnop T, Phatsara M, Chomdej S (2016b) Differences in osteon structure histomorphometry between Golden Retriever puppy and adult stages. Anat Sci Int. doi:10.1007/s12565-016-0345-y

Nielsen FH (1991) Nutritional requirements for boron, silicon, vanadium, nickel, and arsenic: current knowledge and speculation. FASEB J 5:2661–2667

Nielsen FH, Zimmerman TJ, Shuler TR, Brossart B, Uthus EO (1989) Evidence for a cooperative metabolic relationship between Nickel and vitamin B12 in rats. J Trace Elem Exp Med 2:21–29

Panagiotopoulou O, Pataky TC, Hill Z, Hutchinson JR (2012) Statistical parametric mapping of the regional distribution and ontogenetic scaling of foot pressures during walking in Asian elephants (*Elephas maximus*). J Exp Biol 215:1584–1593

Pankovich AM, Simmons DJ, Kulkarni VV (1974) Zonal osteons in cortical bone. Clin Orthop Relat Res 100:356–363

Parkpian P, Leong ST, Laortanakul P, Thunthaisong N (2003) Regional monitoring of lead and cadmium contamination in a tropical grazing land site, Thailand. Environ Monit Assess 85:157–173

Poonkothai M, Vijayavathai BS (2012) Nickel as an essential element and a toxicant. IJES 1:285–288

Rey C, Combes C, Drouet C, Glimcher MJ (2009) Bone mineral: update on chemical composition and structure. Osteoporos Int 20:1013–1021

Roth VL (1984) How elephants grow: heterochrony and the calibration of developmental stages in some living and fossil species. J Vert Paleont 4:126–145

Seeman E (2006) Bone structure and strength. In: Seibel M, Robins SP, Bilezikian JP (eds) Dynamics of bone and cartilage metabolism. Academic, London, pp 213–220

Shil SK, Quasem MA, Rahman ML, Kibria ASMG, Uddin M, Ahasan ASML (2013) Macroanatomy of the bones of pelvis and hind limb of an Asian elephant (*Elephas maximus*). Int J Morphol 31:1473–1478

Skedros JG, Sorenson SM, Jenson NH (2007) Are distributions of secondary osteon variants useful for interpreting load history in mammalian bones? Cells Tissues Organs 185:285–307

Smuts MM, Bezuidenhout AJ (1993) Osteology of the thoracic limb of the African elephant (*Loxodonta africana*). Onderstepoort J Vet Res 60:1–14

Smuts MM, Bezuidenhout AJ (1994) Osteology of the pelvic limb of the African elephant (*Loxodonta africana*). Onderstepoort J Vet Res 61:51–66

Todd NE (2010) Qualitative comparison of the cranio-dental osteology of the extant elephants, Elephas Maximus (*Asian elephant*) and Loxodonta africana (*African elephant*). Anat Rec (Hoboken) 293:62–73

Tzaphidou M, Zaichick V (2004) Sex and age related Ca/P ration in cortical bone of iliac crest of healthy humans. J Radioanal Nucl Chem 259:347–349

van der Merwe NJ, Bezuidenhout AJ, Seegers CD (1995) The skull and mandible of the African elephant (*Loxodonta africana*). Onderstepoort J Vet Res 62:245–260

Weissengruber GE, Egger GF, Hutchinson JR et al (2006) The structure of the cushions in the feet of African elephants (*Loxodonta africana*). J Anat 209:781–792

Wopenka B, Pasteris JD (2005) A mineralogical perspective on the apatite in bone. Mat Sci Eng C25:131–143

Yamaguchi M, Sugii K, Okada S (1982) Tin decreases femoral calcium independently of calcium homeostasis in rats. Toxicol Lett 10:7–10

Zougrou IM, Katsikini M, Pinakidou F, Paloura EC, Papadopoulou L, Tsoukala E (2014) Study of fossil bones by synchrotron radiation micro-spectroscopic techniques and scanning electron microscopy. J Synchrotron Radiat 21:149–160